

The Design, Synthesis, and Property Investigation of Multi-Functional Materials with Aggregation Induced Emission Property and Mechanochromic Luminescent Property

Group Members:

Yuxin Ji

Shuohong Liu

Chen Gao

Instructor:

Mingjun Teng

School:

Beijing National Day School

Location:

Beijing, China

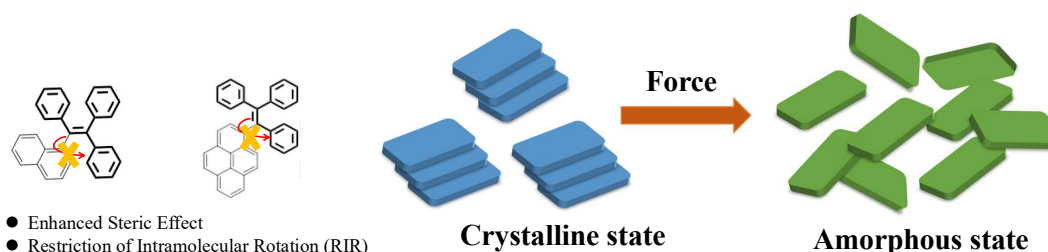
Abstract

We exploit the Classical Suzuki Coupling reaction to tailor the Triphenylethylene group with Naphthalene and Pyrene moieties and manage to obtain the targeted molecule **1** and **2**, which both show aggregation induced emission (AIE) property and mechanochromic luminescent (ML) behavior.

The AIE property is demonstrated by varying the H₂O fraction of **1** and **2** solutions in THF/H₂O mixture (THF: Good solvent/H₂O: Poor solvent). The generated aggregates of **1** from 90% H₂O volume fraction solution shows three times higher emission intensity than that in THF solution, indicating the enhanced fluorescent quantum yield in solid state than that in molecularly dissolved solution. The aggregates of **2** with a bulkier pyrene even show a more significantly intensified luminescent intensity.

The exciting mechanochromic luminescent behaviors are observed and verified. The emission band of as-prepared powder **1** is at 469 nm. After shearing, the emission peak blue-shifted to 466 nm. A more obvious shift is detected for the powder of **2** after shearing, with the emission band changing from 472 nm to 478 nm.

The experiment results indicate the feasibility of our designing principle and demonstrate that the incorporation of bulky conjugated group into triphenylethylene group can endow a single molecule with both aggregation induced emission property and force responsive property. This effective design strategy paved the road for the designing of multi-functional materials.



1 Introduction

The development of multi-functional materials is highly desirable due to its wide applications in real life. [1-9] Recently, smart fluorescent materials have been applied to different areas and have attracted great attentions due to its low cost, tailorable property, and quick response to stimuli. Two newly emerging smart luminescent materials are the mechanochromic luminescent (ML) material and the aggregation induced emission (AIE) material.

The ML material is force-responsive and can change emission property when imposing external pressure, shearing, or grinding. ML materials are the promising candidates that could be used in mechanical sensing, bio-imaging, and data storage device. [10-14]

Common luminescent materials are suffering from notorious aggregation caused quenching (ACQ) phenomenon; that is, their emission intensity is quite low in solid state. In contrast, the AIE materials have a much higher fluorescent quantum yield in the aggregated state than that of solution. Due to the high emission efficiency, AIE materials are quite advantageous in practical use due to their low cost. [15-19]

Smart materials with both ML and AIE property are highly desirable while there are not so many successful examples. Especially, the effective designing principle and clear structure-property relationship have not been established yet. Thus, it is essentially important to build up the molecular designing strategy and put them in to practice.

Triphenylethylene is a quite useful scaffold for constructing AIE materials. Base on this feature, our molecular design strategy is to tailor the Triphenylethylene with conjugated and rigid chromophore, such as Naphthalene and Pyrene. On one hand, the bulky Naphthalene and Pyrene can restrict intramolecular rotation (RIR) and prohibit the non-radiative relaxation, which are helpful for generating the AIE behavior. On the other hand, the planar and rigid Naphthalene and Pyrene can guarantee a good crystallinity of the molecules, which is essential for ML property because the

common mechanism for ML materials are based on crystalline-to-amorphous transition.

Our purpose is to create new types of luminescent materials that combine the ML and AIE properties in the same molecule and further establish a clear relationship between molecular structures and their properties. Such multi-functional materials contribute to fundamental research and practical applications such as anti-counterfeit, wind tunnel experiment, and strain analysis of architecture. Particularly, due to its high fluorescent quantum yield in the solid state, such materials demonstrate their advantage in real-life applications because of their low cost.

2 Experiments

2.1 Reagents

Reagent	Reagent Specification	Manufacturer
Na ₂ CO ₃	Analytical Reagent (A.R.)	Sinopharm Chemical Reagent Beijing Co., Ltd
Triphenylethylene	Chemical Pure (C. R.)	Prior preparation
Pd(PPh ₃) ₄	A.R.	Sigma-Aldrich
THF	A.R.	Sinopharm Chemical Reagent Beijing Co., Ltd
petroleum	A.R.	Sinopharm Chemical Reagent Beijing Co., Ltd
chloroform	A.R.	Sinopharm Chemical Reagent Beijing Co., Ltd
dichloromethane	A.R.	Sinopharm Chemical Reagent Beijing Co., Ltd
1-naphthaleneboronic acid	A.R.	Sigma-Aldrich Co.
1-pyrenylboronic acid	A.R.	Sigma-Aldrich Co.

2.2 Instrument

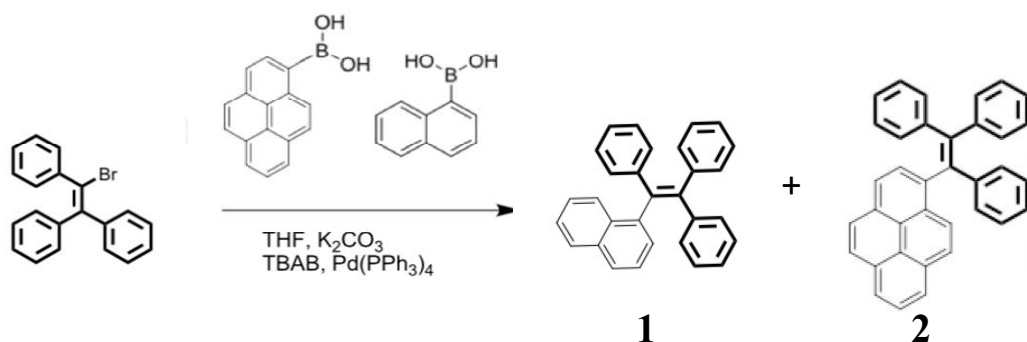
Nuclear Magnetic Resonance (NMR): ¹H NMR was recorded on 400 MHz (Bruker: ARX400) at room temperature using the CDCl₃ as the solvents and the tetramethylsilane (TMS) as the internal standard.

Mass Spectrum (MS): the molecular weight of the compound was acquired by the Bruker Apex IV FTMS mass spectrometer in the positive and high resolution mode.

Fluorescence spectra was recorded on F7000 fluorescence spectrophotometer. The quartz cuvettes used for measurement were of 1 cm length.

UV vis spectrum was obtained on Lambda 35 Perkin Elmer.

2.3 Synthetic Route



Scheme 1. Synthesis of **1** and **2**

2.4 Procedure

2.4.1 Synthesis of **1**

The Triphenylethylene (427 mg, 1.1 eq) and 1-naphthaleneboronic acid (200 mg, 1.2 eq) was dissolved in the solvent THF, with Pd(PPh₃)₄ (30 mg) and water (0.2 mL) as catalysts, which were later refluxed at 90°C for 12 hours under the N₂ protection. After the solvent was evaporated, the residue was purified by silicon column separation with petroleum/CH₂Cl₂=10:1.

The obtained sample emitted blue fluorescence under the UV radiation.



Figure 1. Powder of **1** under the UV radiation

2.4.2 Synthesis of 2

The Triphenylethylene (335 mg, 1.0 eq) and 1-naphthaleneboronic acid (295 mg, 1.2 eq) were dissolved in THF with Pd(PPh₃)₄ (34.7 mg, 0.03 eq) and water (0.6 mL) as catalysts, which were refluxed at 80 for 12 hours under the N₂ protection. After the solvent was evaporated, light yellow powder was obtained and further purified by silicon column separation with petroleum/CH₂Cl₂=10:1.

The obtained sample emitted blue-green fluorescence under the UV radiation.



Figure 2. As prepared powder 2 **Figure 3.** As prepared powder 2 under UV light

2.5 Verification of Molecular structure

2.5.1 Sample 1

(1) Nuclear Magnetic Resonance spectrum

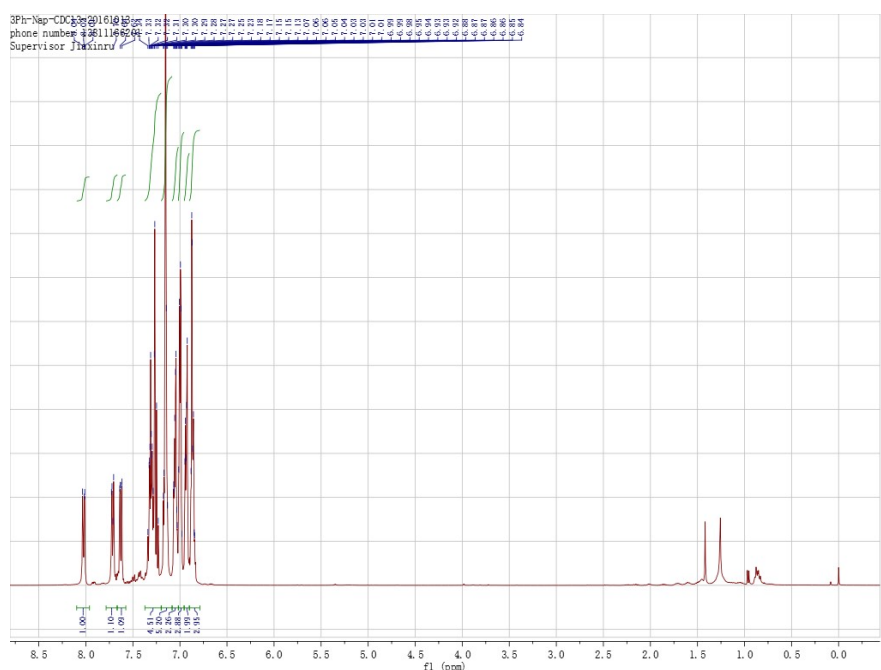


Figure 4. NMR of 1 in CDCl₃

^1H NMR (CDCl_3 , 500M) ppm: 8.04-8.00 (dd, 1H), 7.67-7.65(dd, 1H), 7.63-7.62 (dd, 1H), 7.33-7.23 (m, 5H), 7.18-7.13(m, 6H), 7.07-7.03 (m, 2H), 7.01-6.98(m, 2H), 6.96-6.92 (m, 2H), 6.88-6.84(m, 2H)

(2) Mass Spectrum

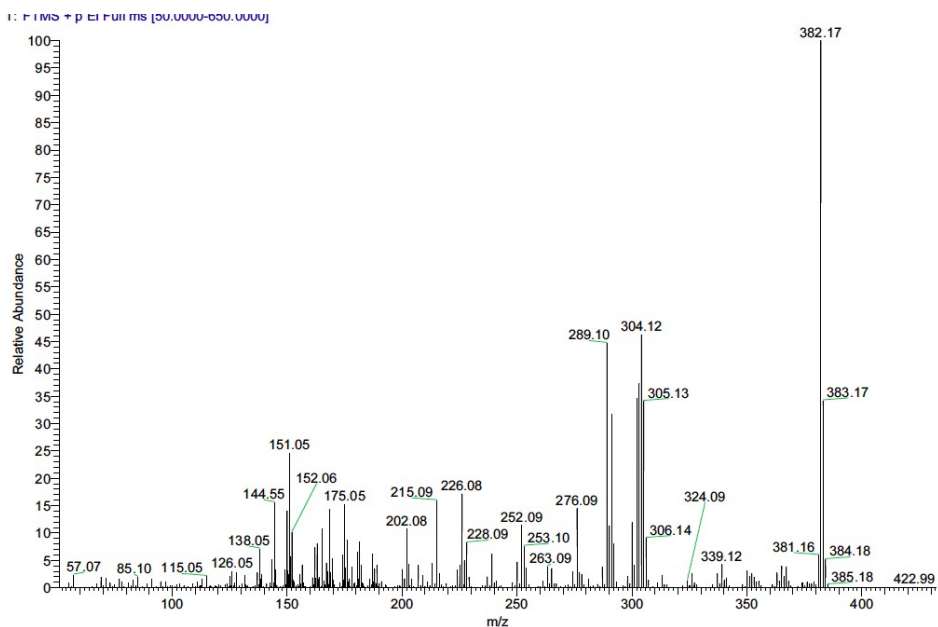


Figure 5. Mass spectrum of **1**

Calcd. For $\text{C}_{30}\text{H}_{22}$: 382.17 Found $[\text{M}]^+$: 382.17

2.5.2 Sample 2

(1) Nuclear Magnetic Resonance spectrum

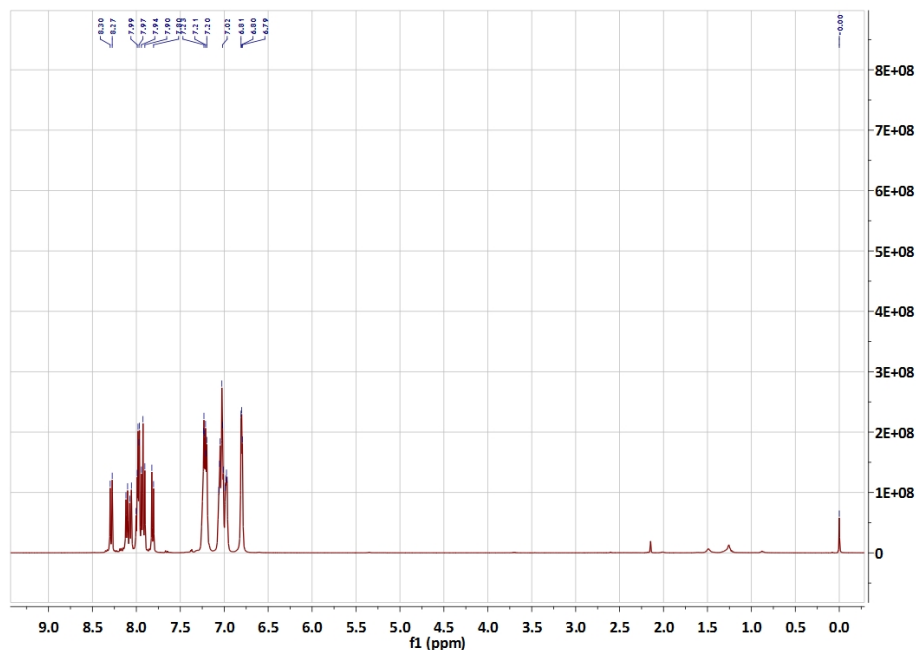


Figure 6. NMR of **2** in CDCl_3

^1H NMR (CDCl_3 , 500M) ppm: 8.30-8.27(d, 1H), 8.12-8.10 (d, 1H), 8.07-8.06(d, 1H), 7.97-7.90 (m, 4H), 7.82-7.80 (d, 1H), 7.23-7.20 (m, 6H), 7.05-6.97 (m, 7H), 6.81-6.79 (m, 3H)

(2) Mass Spectrum

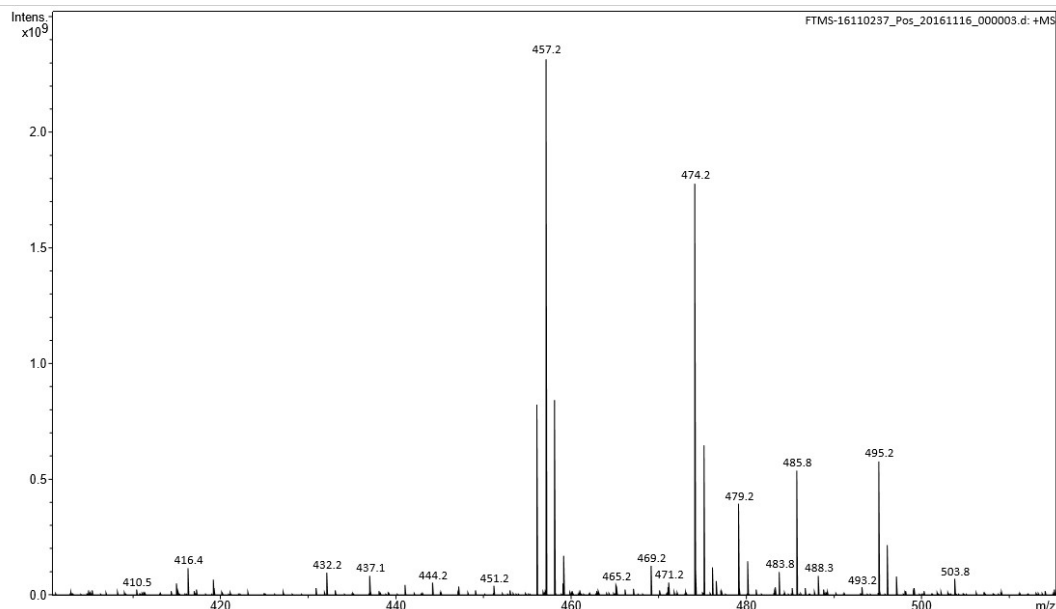


Figure 7. NMR of **2** in CDCl_3

Calcd. For $\text{C}_{36}\text{H}_{24}$: 456.6 Found $[\text{M}+\text{H}]^+$: 457.2

2.6. Sample preparation for AIE property measurement of **1** and **2**

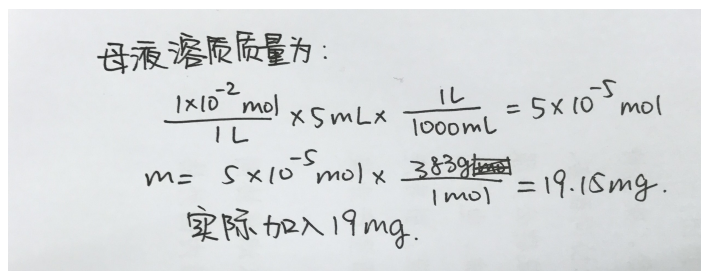
Compound **1** and **2** show a good solubility in organic solvent, such as THF, dichloromethane, chloroform, while they are poorly soluble in H_2O . Thus, the precipitation method was applied to generate the aggregates by using THF and H_2O mixture as the solvent.

Typical procedure is as follows:

a. **1** or **2** was dissolved in THF to prepare 5×10^{-5} mol/L stock solution.

b. 50 μL stock solution was quickly injected by pipette into vigorously stirring 10 mL solution with different THF/ H_2O ratios (H_2O volume fraction ranges from 0 % to 100 %). The solution was set aside for 1 hour before fluorescent measurement.

For **1**, 5 mL of stock solution was prepared for the compound. According to calculation, 19.15 mg of sample was required; 19.00 mg of the sample was added in reality.



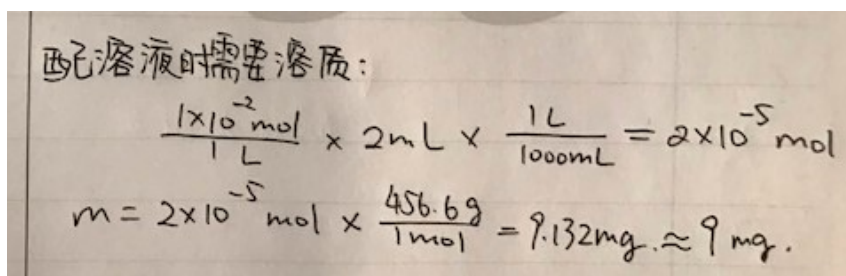
母液溶质质量为:

$$\frac{1 \times 10^{-2} \text{ mol}}{1 \text{ L}} \times 5 \text{ mL} \times \frac{1 \text{ L}}{1000 \text{ mL}} = 5 \times 10^{-5} \text{ mol}$$
$$m = 5 \times 10^{-5} \text{ mol} \times \frac{383.9 \text{ g}}{1 \text{ mol}} = 19.15 \text{ mg.}$$

实际加入 19 mg.

Figure 8. The calculation process for preparing stock solution of **1**

For **2**, 2 mL of stock solution was prepared for the compound. According to calculation, 9 mg of sample was acquired; 9.18 mg of the sample was added in reality.



配溶液时需要溶质:

$$\frac{1 \times 10^{-2} \text{ mol}}{1 \text{ L}} \times 2 \text{ mL} \times \frac{1 \text{ L}}{1000 \text{ mL}} = 2 \times 10^{-5} \text{ mol}$$
$$m = 2 \times 10^{-5} \text{ mol} \times \frac{456.6 \text{ g}}{1 \text{ mol}} = 9.132 \text{ mg.} \approx 9 \text{ mg.}$$

Figure 9. The calculation process for preparing stock solution of **2**

3 Result and Analysis

3.1 Aggregation induced emission (AIE) behaviors

3.1.1 AIE behavior of **1**

To get the information of AIE phenomenon of **1**, we turned to the emission behaviors of **1** aggregates from the THF/H₂O mixture in which THF is good solvent for **1** while **1** is barely soluble in H₂O. It is expected that **1** will form aggregates when increasing the H₂O volume fraction to certain extent, accompanying with variation of emission property.

As shown in **Figure 10**, when **1** is dissolved in the good solvent THF with molecularly dispersed state, weak blue luminescence can be observed under UV light (365 nm) irradiation. Gradually increasing water fraction results in intensified blue-green luminescence.

Fluorescent spectra further evident the change of emission property. The emission band of **1** in THF solution centered at 370 nm, and a new emission peak at 477 nm appeared when water fraction (f_w , by volume) increases from 60% to 70%.

Further increasing f_w to 90% led to a dramatically enhanced emission at 490 nm, which is 3 times higher than that in pure THF solution.

As displayed in **Figure 11**, the monitoring of emission band 370 nm and 477 nm revealed that 370 nm emission intensity gradually quenched with increasing f_w from 0% to 90%, while the emission band at 477 nm dramatically jumped from zero to 300 times higher levels at high H₂O volume fraction. The above result verified the AIE behaviors of **1**.

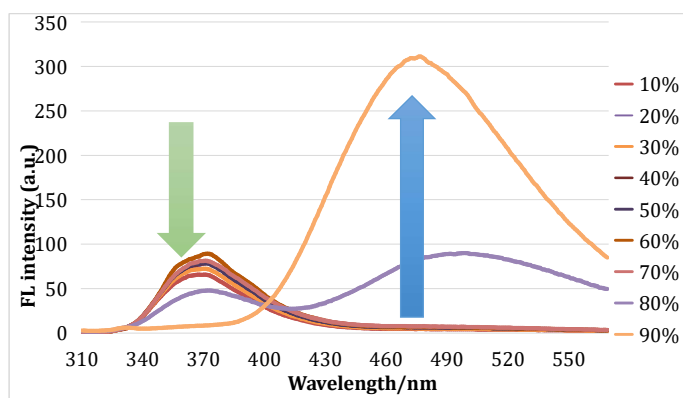
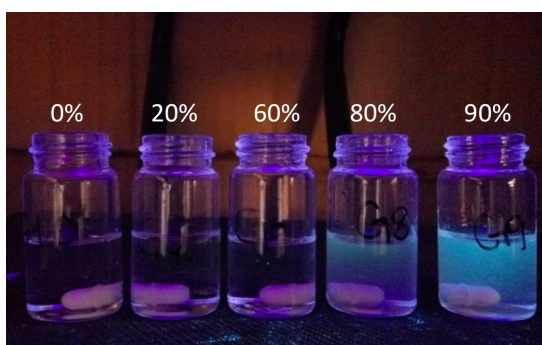


Figure 10. (Left): Picture of **1** solution of different water content ratio under ultraviolet light; (Right): fluorescent spectra of **1** solution with of different water content ratios.

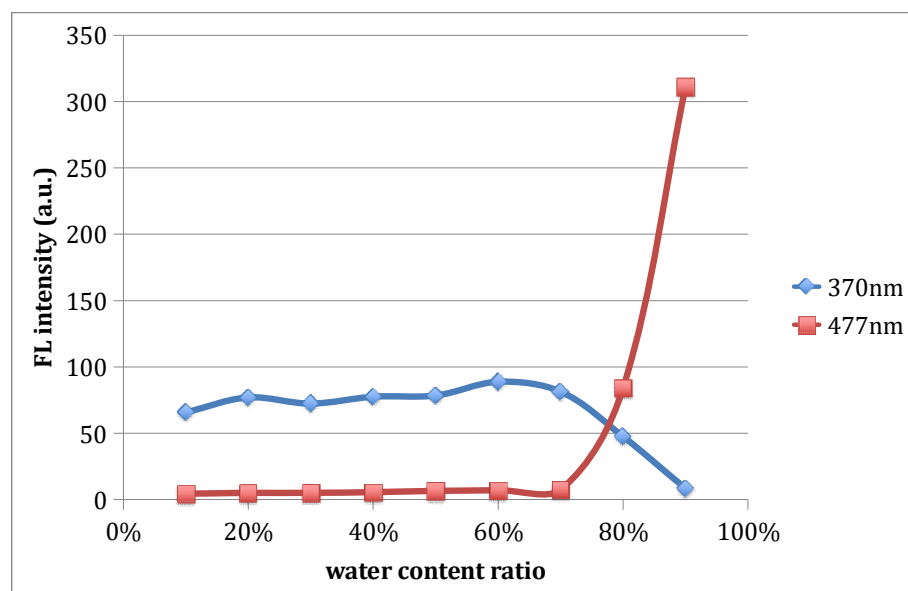


Figure 11. The relationship between fluorescent emission intensity and H₂O fractions.

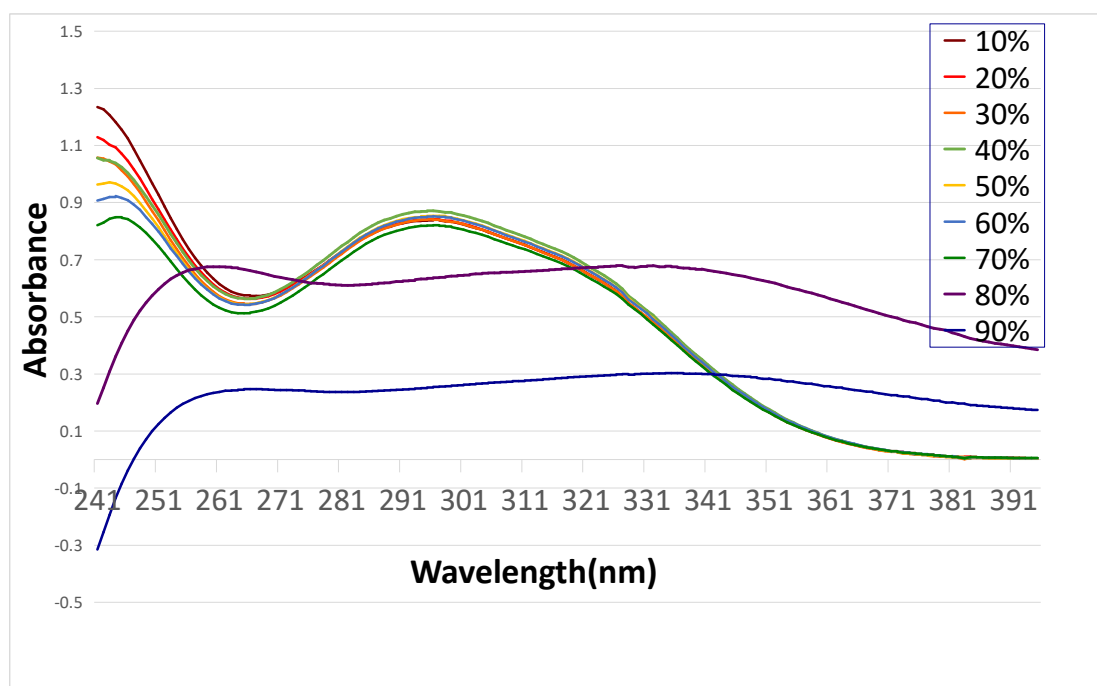


Figure 12. UV-vis spectra of **1** solution with of different water content ratios

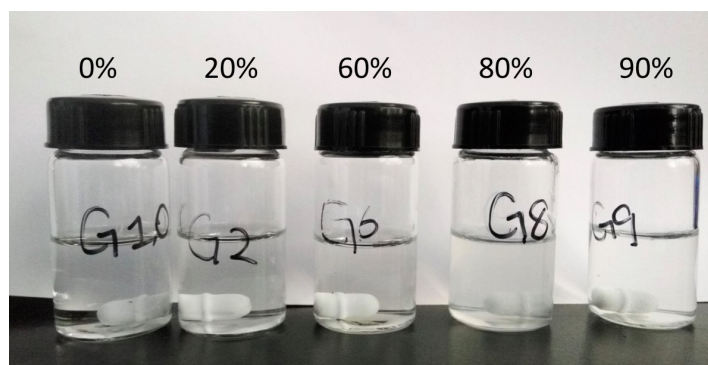


Figure 13. Picture of **1** solution with of different water content ratio.

The UV-vis spectrum of **1** conveyed useful information for the formation of aggregates (Figure 12). When increasing water fraction, the red-shift of absorption band from 296 nm to 335 nm indicated the interaction of chromophores resulted from closer distance, demonstrating the formation of aggregates. For higher H₂O fraction (80% and 90%), a leveling-off absorption band was detected in the ultraviolet regions, which is a feature of aggregates suspension.

For naked-eye observation of the solutions with water fraction ranging from 0% to 70%, the vial is found to be homogeneous and transparent, which suggest there are no aggregates in a nanoscale (Figure 13). The solution turns to turbid for high water

fraction (80%-90%), an indication of forming of large-scale aggregates.

Supported by the fluorescent data and UV-vis absorption result, the emission band at 370 nm can be assigned to the monomeric emission band while the broader and less structured emission at longer wavelength 477 nm is an indicative of a more-conjugated emissive species. The shift of emission band can be attributed to the restriction of intramolecular rotations when forming the aggregates in THF/H₂O mixture. In addition, the aggregates suspension of **1** has a red shift of absorption peak when compared with that of the molecular dispersed solution. Such change indicates that there may be an extension of conjugation in the aggregates, which may result from the planarization of the twist and the bulky group.

The above results clearly demonstrated that **1** display AIE behavior, which is also supported by the strong fluorescence of as-prepared powder of **1** (**Figure 14**).



Figure 14. The powder **1** emitted strong fluorescent under ultraviolet light.

3.1.2 AIE phenomenon of **2**

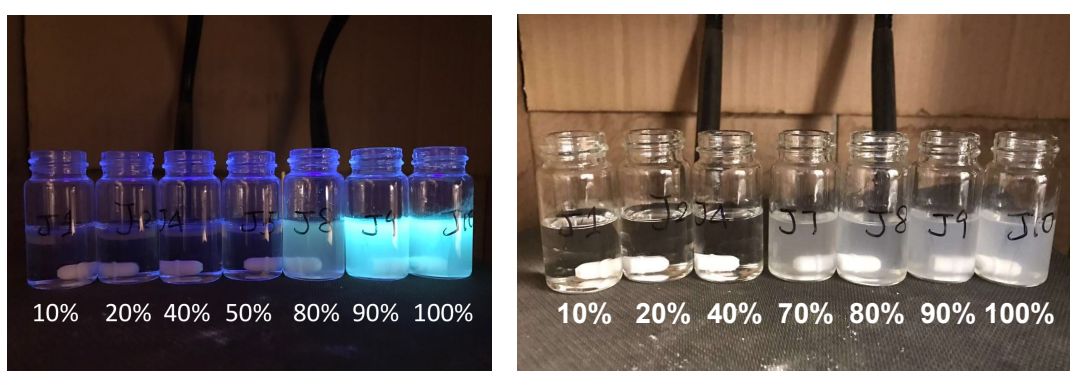


Figure 15. **2** solutions with different water content ratios under UV light (left) and visible light (right).

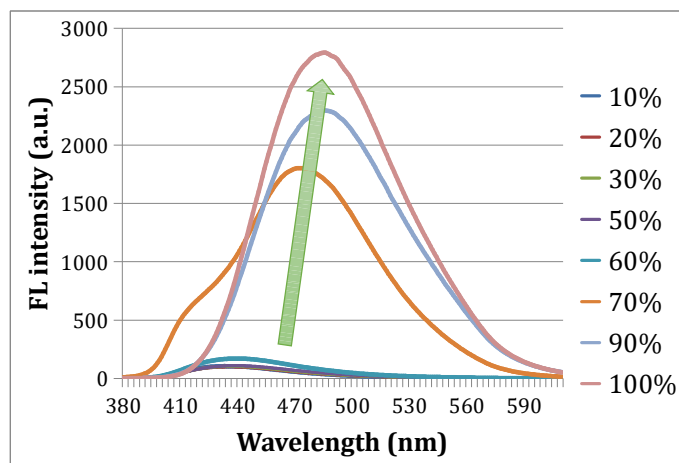


Figure 16. The fluorescence spectra of **2** solution of different water content ratios

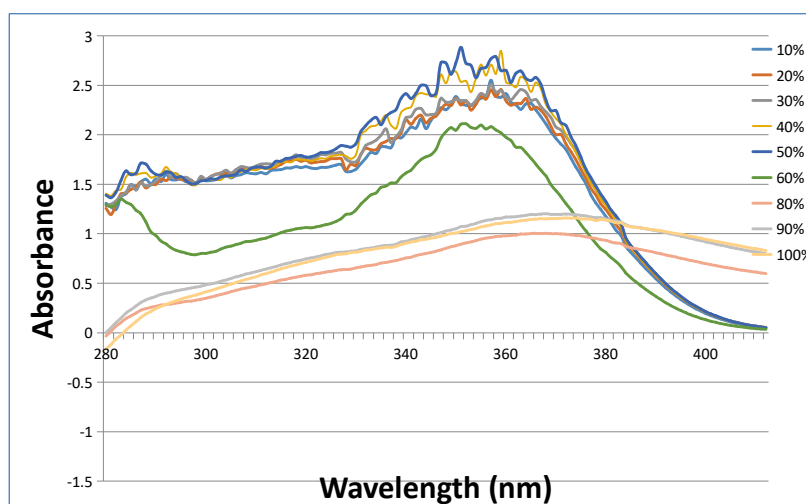


Figure 17. UV-vis spectra of **2** solution with of different water content ratios

The AIE behaviors of **2** are also investigated in the solution of THF/H₂O miscible solution. As displayed in **Figure 15**, as the ratio of H₂O increases, the fluorescence intensity of the solution becomes more intensive, suggesting the AIE nature of the sample. Presented by the fluorescence spectra (**Figure 16**), the emission peak of the sample in THF (without H₂O) is approximately 450 nm, but its luminescence intensity is negligible. As the H₂O ratio increased up to 70%, a new band with much stronger intensity at longer wavelength, 470 nm, appeared. When the water content ratio rises from 90% to 100%, the intensity of the 486 nm emission band significantly increased, suggesting its good aggregation-induced emission property. The red-shift and intensive emission band were primarily due to the

restriction intramolecular rotation (RIR) and a more conjugated structure in aggregated state. The picture and UV-vis spectra further revealed the formation of aggregates when f_w is above 70%, which confirm that the intensified emission correlates to the forming of aggregation. In addition, as-prepared powder of **2** emitted strong fluorescents under UV light, which supported the conclusion made about its aggregation-induced fluorescent property (see **Figure 17**).

Compared to **1**, compound **2** has a more significant AIE effect. The emission intensity of $f_w = 90\%$ for **1** is 3-fold than that in THF ($f_w = 0\%$). While for **2**, there are almost 22-fold increase in the same condition, which may result from the fact that **2** have a bulkier pyrene group that help restrict the single bond rotation.

3.2 The mechanochromic luminescent property

3.2.1 The mechanochromic luminescent property of Sample 1

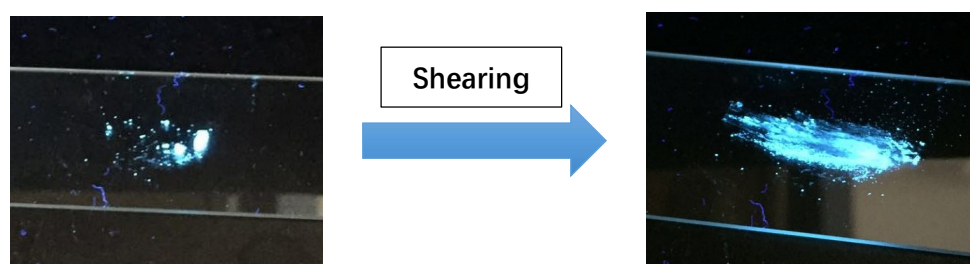


Figure 18. Powder **1** before and after shearing under UV light radiation.

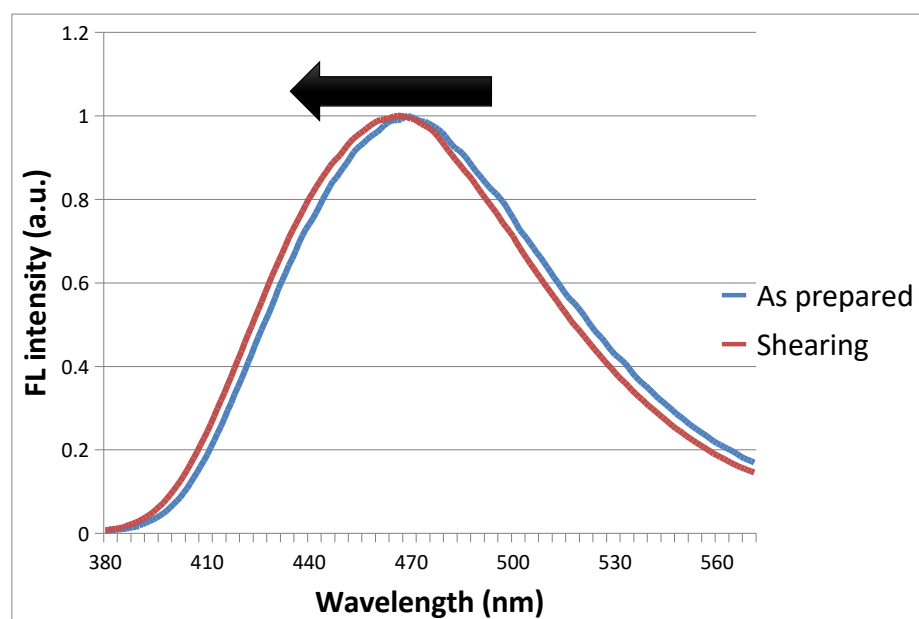


Figure 19. Fluorescent spectra of powder **1** before and after shearing

In order to further explore the mechanochromic luminescent property of the sample **1**, we pry into the change of emission property before and after shearing (**Figure 18**).

In the normalized fluorescent spectra as shown in the **Figure 19**, the orange and blue curves represent **1** before and after shearing respectively. The emission peak of the as-prepared powder centered at 469 nm. After shearing, the emission band blue-shifted to 466 nm. The blue-shift of 3 nm demonstrated that force will influence the fluorescent properties of **1**.

3.2.2 The mechanochromic luminescent property of Sample 2

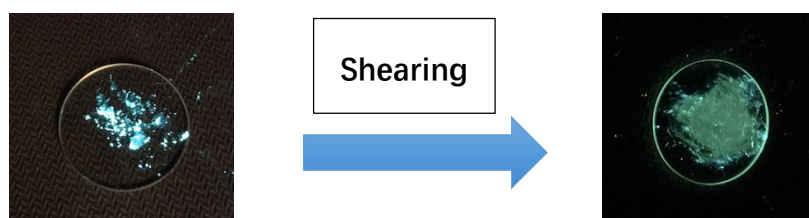


Figure 20. Powder **2** before and after shearing under UV radiation

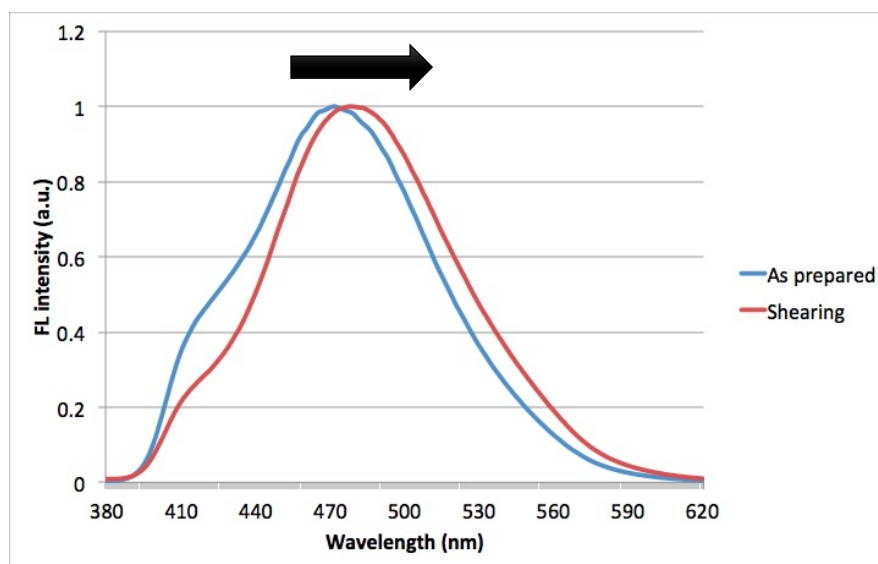
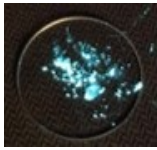
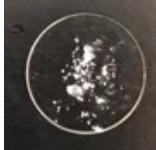
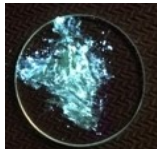
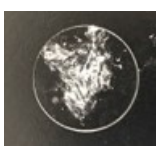
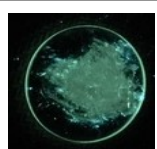


Figure 21. Fluorescent spectra of powder **2** before and after shearing

Compared to **1**, **2** displays a more significant mechanochromic luminescent behavior. The powder obtained from column purification exhibited blue-green light under 365 nm UV-irradiation. After slightly shearing by spatula, the luminescent color changed to deep green (**Figure 20**).

Fluorescent spectra provide quantitative evidence of force-responsive behaviors. As displayed in **Figure 21**, as-prepared powder showed the emission peak at 472 nm with a shoulder band at around 410 nm. After shearing, the emission band red-shifted to 478 nm and the shoulder peak at 410 nm decreased correspondingly. The change of emission band of **2** (6 nm red-shift) is more obvious than that of **1**.

Table 1. The emission color change of **2** under different force perturbations.

State of 2	Under the UV radiation	Observed by Naked-eye
Before shearing		
After slightly shearing		
further shearing		

3.3 Mechanism

(1) Aggregation-induced emission property

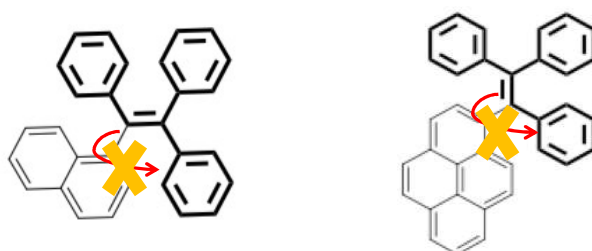
Rigid group Naphthalene and Pyrene chromosphere was introduced to the triphenylethylene skeleton for the target sample **1** and **2**, therefore enhancing the steric effect:

a. In good solvent THF, the compound was at the state of a single molecule, allowing the groups (such as Naphthalene, Pyrene or Benzene) that are connected to double bonds to rotate freely.

b. With the introduction of poor solvent H₂O, the solubility of the compound decreased and it transited from the molecularly dispersed state to the aggregation state (e.g. solid), which restricted the self-rotation of the intramolecular group, decreasing the energy consume caused by single-bond rotation and the molecule's non-radiative relaxation. Thus, it allowed more energy to be used for generating fluorescence, and therefore enhanced the quantum yield of the sample (**Figure 22**). Consequently,

according to the observation in the experiment, when the H₂O content ratio reaches a certain degree (70%), aggregates were formed and the fluorescent intensity was significantly enhanced.

Since the pyrene moiety in **2** is bulkier than naphthalene in **1**, it is reasonable that **2** exhibits a more intensive AIE behavior with 22-folds enhanced fluorescent in aggregation state than that in THF solution, while **1** is 3-folds stronger in the same condition. The result above suggested that introducing bulky group can be an effective way to improve AIE behaviors.



- Enhanced Steric Effect
- Restriction of Intramolecular Rotation (RIR)

Figure 22. The restriction of intramolecular rotation of **1** and **2**.

(2) Macheochromic property

Targeted sample **1** and **2** are constructed by the rigid and planar groups such as vinyl unit, benzene, naphthalene or pyrene groups, which endowed the molecules with good crystallinity in solid state. External force, such as shearing and grinding, is capable to break down the crystalline state into amorphous state (**Figure 23**). In these two different states, the self-assembled microstructures are quite distinct and the chromophores adopted different packing mode. For sample **1**, shearing destroyed the original packing style to a less conjugated structure which corresponding to blue-shift of emission band. In contrast, **2** undergoes a transition from a twisted structure to a more conjugated packing style, which is evidenced by the 6 nm red-shift in fluorescent spectra.

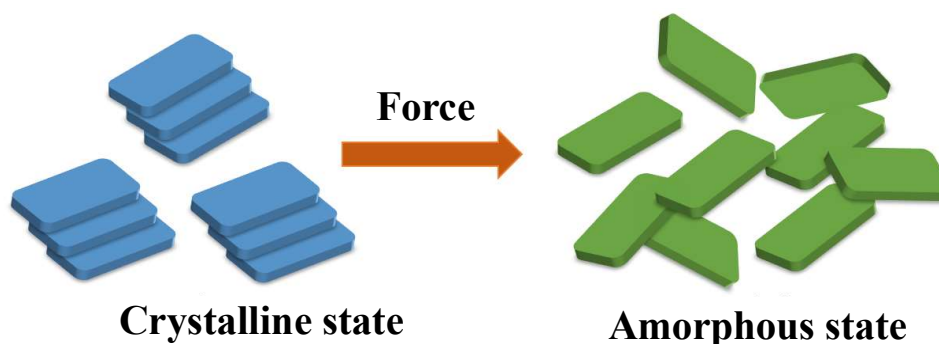


Figure 23. The mechanism of mechanochromic behavior of **1** and **2**.

4 Conclusion

Luminescent materials that have both aggregation induced emission (AIE) property and mechanochromic luminescent (ML) properties are successfully synthesized by combining naphthalene and pyrene with Triphenylethylene.

When the proportion of poor solvent H₂O was above 80%, aggregates composed of molecules **1** and **2** were forming and exhibiting much higher emission intensity than that in the THF solution. The aggregated state restricts the rotation of the bulky chromophores and prohibit the radiation energy loss caused by the intramolecular single bond rotation, which enhanced their fluorescent quantum yield. Due to the bulkier pyrene group, **2** showed a more significant AIE behavior (20-folds enhancement) than **1** (3-folds enhancement).

In addition, force can break the original microstructures of the molecules **1** and **2** in solid state and change its self-assembled arrangements, which led to the shift of emission band. Under force perturbation, emission band of **1** was blue-shifted while that of **2** was red-shifted.

This kind of organic materials has a wide range of applications such as anti-counterfeiting, architecture damage detects, and wind tunnel experiment. Especially, the cost of production is lowered because fewer materials are needed, and the AIE property guarantees high luminescent quantum yield of the materials in solid state. Therefore, this material is very competitive in application as well as in the material market. It also provides new ideas for future research.

5 Reference

- [1] Bellomo E.G. , Wyrsta M.D. , Pakstis L. , Pochan D. J. , Deming T. J. Stimuli-responsive Polypeptide Vesicles by Conformation-specific Assembly. *Nat. Mater.* **2004**, *3*, 244–248.
- [2] de Loos, M.; Feringa, B. L.; van Esch, J. H. Design and Application of Self-Assembled Low Molecular Weight Hydrogels. *Eur. J. Org. Chem.* **2005**, *17*, 3615–3631.
- [3] Ishi-I, T.; Shinkai, S. Dye-Based Organogels Stimuli-Responsive Soft Materials Based on One-Dimensional Self-Assembling Aromatic Dyes. *Top. Curr. Chem.* **2005**, *258*, 119–160.
- [4] van Bommel, K. J. C.; van der Pol, C.; Muizebelt, I.; Friggeri, A.; Heeres, A.; Meetsma, A.; Feringa, B. L.; van Esch, J. Responsive Cyclohexane-Based Low-Molecular-Weight Hydrogelators with Modular Architecture. *Angew. Chem., Int. Ed.* **2004**, *43*, 1663–1667.
- [5] Deindörfer, P.; Davis, R.; Zentel, R. Photoresponsive Anisotropic and Isotropic Gels of Semicarbazide-azobenzene Organogelators the Use of Magnetic Polymer Colloids to Detect Gel–sol Transformation. *Soft Matter.* **2007**, *3*, 1308–1311.
- [6] Tong, X.; Zhao, Y.; An, B. K.; Park, S. Y. Fluorescent Liquid-Crystal Gels with Electrically Switchable Photoluminescence *Adv. Funct. Mater.* **2006**, *16*, 1799–1804.
- [7] Yan, Q.; Yuan, J. Y., Cai, Z. N.; Xin, Y.; Kang, Y.; Yin, Y. W. Voltage-Responsive Vesicles Based on Orthogonal Assembly of Two Homopolymers. *J. Am. Chem. Soc.*, **2010**, *132*, 9268–9270.
- [8] Yan, Q.; Yuan J.Y., Kang, Y., Cai, Z.N., Zhou, L.L., Yin, Y.W. Dual-sensing Porphyrin-containing Copolymer Nanosensor as Full-spectrum Colorimeter and Ultra-sensitive Thermometer. *Chem. Commun.* **2010**, *46*, 2781–2783.
- [9] Wang, S.; Todd, E. K.; Birau, M.; Zhang, J.; Wan, X.; Wang, Z. Y. Near-Infrared Electrochromism in Electroactive Pentacenediquinone-Containing Poly(aryl ether)s. *Chem. Mater.* **2005**, *17*, 6388–6394.

- [10] Sagara, Y.; Kato, T. Stimuli-responsive Luminescent Liquid Crystals Change of Photoluminescent Colors Triggered by a Shear-induced Phase Transition. *Angew. Chem. Int. Ed.* **2008**, *47*, 5175–5178.
- [11] Sagara, Y.; Yamane, S.; Mutai, T.; Araki, K.; Kato, T. A Stimuli-Responsive, Photoluminescent, Anthracene-Based Liquid Crystal Emission Color Determined by Thermal and Mechanical Processes. *Adv. Funct. Mater.* **2009**, *19*, 1869–1875.
- [12] Sagara, Y.; Kato, T. Brightly Tricolored Mechanochromic Luminescence from a Single-Luminophore Liquid Crystal Reversible Writing and Erasing of Images. *Angew. Chem. Int. Ed.* **2011**, *50*, 9128–9132.
- [13] Kozhevnikov, V. N.; Donnio, B.; Bruce, D. W. Phosphorescent, Terdentate, Liquid-crystalline Complexes of Platinum(II) Stimulus-dependent Emission. *Angew. Chem. Int. Ed.* **2008**, *47*, 6286–6289.
- [14] Lee, W.-E.; Lee, C.-L.; Sakaguchi, T.; Fujiki, M.; Kwak, G. Piezochromic Fluorescence in Liquid Crystalline Conjugated Polymers. *Chem. Commun.* **2011**, *47*, 3526–3528.
- [15] Cheng, J.; Liang, X.; Cao, Y.; Guo, K.; Wong, W.-Y., Aldehyde end-capped terthiophene with aggregation-induced emission characteristics. *Tetrahedron*, **2015**, *71*, 5634-5639.
- [16] Wang, A.; Yang, Y.; Yu, F.; Xue, L.; Hu, B.; Fan, W.; Dong, Y., A highly selective and sensitive fluorescent probe for quantitative detection of Hg²⁺ based on aggregation-induced emission features. *Talanta*, **2015**, *132*, 864-870.
- [17] Rananaware, A.; La, D.D.; Bhosale, S.V., Aggregation-induced emission of a star-shape luminogen based on cyclohexanehexone substituted with AIE active tetraphenylethene functionality. *Rsc Advances*, **2015**, *5*, 56270-56273.
- [18] Mazumdar, P.; Das, D.; Sahoo, G.P.; Salgado-Moran, G.; Misra, A., Aggregation induced emission enhancement of 4,4'-bis(diethylamino)benzophenone with an exceptionally large blue shift and its potential use as glucose sensor. *Physical Chemistry Chemical Physics*, 2015, *17*, 3343-3354.
- [19] Ezhumalai, Y.; Wang, T.-H.; Hsu, H.-F., Regioselective Synthesis of Tetraphenyl-1,3-butadienes with Aggregation-Induced Emission. *Organic*

Letters, **2015**, *17*, 536-539.